Measurement of Temporal Correlations of the Overhauser Field in a Double Quantum Dot

D. J. Reilly,[1,*] J. M. Taylor,[2] E. A. Laird,[1] J. R. Petta,[3] C. M. Marcus,[1] M. P. Hanson,[4] and A. C. Gossard[4]

[1]*Department of Physics, Harvard University, Cambridge, Massachusetts 02138, USA*
[2]*Department of Physics, Massachusetts Institute of Technology, Cambridge, Massachusetts 02139, USA*
[3]*Department of Physics, Princeton University, Princeton, New Jersey 08544, USA*
[4]*Department of Materials, University of California, Santa Barbara, California 93106, USA*

(Received 24 December 2007; published 4 December 2008)

In quantum dots made from materials with nonzero nuclear spins, hyperfine coupling creates a fluctuating effective Zeeman field (Overhauser field) felt by electrons, which can be a dominant source of spin qubit decoherence. We characterize the spectral properties of the fluctuating Overhauser field in a GaAs double quantum dot by measuring correlation functions and power spectra of the rate of singlet-triplet mixing of two separated electrons. Away from zero field, spectral weight is concentrated below 10 Hz, with $\sim 1/f^2$ dependence on frequency f. This is consistent with a model of nuclear spin diffusion, and indicates that decoherence can be largely suppressed by echo techniques.

DOI: 10.1103/PhysRevLett.101.236803 PACS numbers: 73.21.La, 03.67.Lx, 73.63.Kv

Electron spins in quantum dots are an attractive candidate for quantum bits (qubits) [1,2]. For gate-defined devices made using GaAs, the coupling of single electron spins to $\sim 10^6$ thermally excited nuclear spins creates a fluctuating effective Zeeman field (the Overhauser field), $\mathbf{B}_{\mathrm{nuc}}$, with rms amplitude $B_{\mathrm{nuc}} \sim 1$–3 mT [3–7]. At experimentally accessible temperatures, $\mathbf{B}_{\mathrm{nuc}}$ fluctuates both as a function of position and time, with temporal correlations over a broad range of time scales, and is the dominant source of spin dephasing [8–13] and low-field spin relaxation [3,4,7,14–16] in these systems. Spin manipulation schemes [10,17–19] to control spin dephasing, such as spin echo and its generalizations, depend critically on a knowledge of correlations and time scales of the fluctuating nuclear environment.

Previously, fluctuating Overhauser fields have been investigated in atomic systems [20] using optical Faraday rotation, superconducting quantum interference devices [21], and force-detected magnetic resonance [22]. In quantum dots, dynamic nuclear polarization (DNP) [23–26] can drive the nuclear system beyond equilibrium to produce fluctuating currents and feedback effects in connection with Pauli spin blockade [15,27–29].

In this Letter, we report measurements of the temporal correlations and power spectral densities of the nuclear environment in a two-electron GaAs double-quantum-dot system. In contrast to previous work [15,25,26], we do not drive the nuclear system using DNP, but rather probe the statistical fluctuations of the unpolarized nuclear bath in thermal equilibrium [8,12]. Fluctuations of the Overhauser field are detected as fluctuations in the dephasing time of a two-electron spin state, making use of high-bandwidth proximal charge sensing [30]. Fluctuations are found to be broadband over the measurement bandwidth, 40 mHz–1 kHz, and sensitive to an applied magnetic field in the range $B = 0$–20 mT. Experimental results are shown to be consistent with a simple diffusion model of nuclear dynamics, also presented here.

The double quantum dot is formed by Ti/Au top gates on a $GaAs/Al_{0.3}Ga_{0.7}As$ heterostructure with a two-dimensional electron gas (2DEG) with density 2×10^{15} m^{-2} and mobility 20 m^2/Vs, 100 nm below the surface [Fig. 1(a), inset], similar to devices reported previously [9,26]. Measurements are made in a dilution refrigerator with base electron temperature of ~ 120 mK. The conductance G_{QPC} of a proximal radio frequency quantum point contact (rf QPC) is sensitive to the charge configuration of the double dot. G_{QPC} controls the quality factor of a rf tank circuit, modulating the reflected power of a 220 MHz carrier. Demodulation yields a voltage V_{rf}, proportional to G_{QPC}, that constitutes the charge-sensing signal [30]. The applied field B is oriented perpendicular to the 2DEG.

Figure 1(a) shows the relevant energy levels of the double dot in the vicinity of the (2,0)–(1,1) charge transition [first (second) index is the charge in the left (right) dot]. Interdot tunneling t_c and detuning ϵ from the charge degeneracy are determined by electrostatic gates. A gate-pulse [Fig. 1(b)] cycle prepares new singlets each iteration by configuring the device deep in (2,0), at point (P), where transitions to the ground state singlet $(2, 0)S$ occur rapidly [14]. Electrons are then separated to position S in (1,1) for a time τ_S where precession between the initial singlet and one of the triplet states is driven by components of the difference in Overhauser fields in the left and right dots, $\Delta \mathbf{B}_{\mathrm{nuc}} = \mathbf{B}^l_{\mathrm{nuc}} - \mathbf{B}^r_{\mathrm{nuc}}$ [9,13].

In an applied field, the position of the separation point determines whether the (1,1) singlet (S) is nearly degenerate with one of the (1,1) triplets, with which it can then rapidly mix. Mixing of S with T_0 (the $m_s = 0$ triplet) occurs at large negative ϵ [left (green) dashed line in Fig. 1(b)] where exchange vanishes. S-T_0 mixing is driven

 © 2008 The American Physical Society

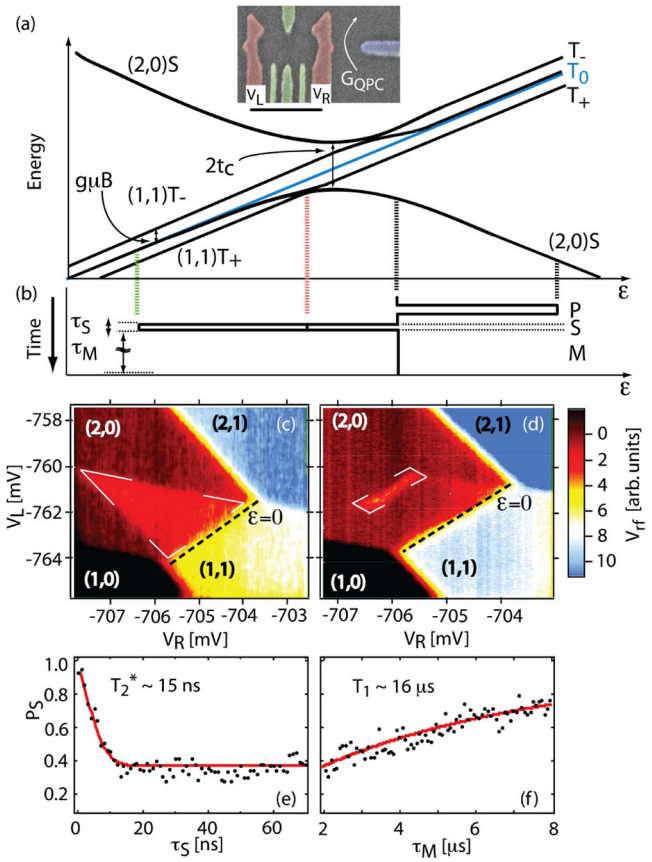

FIG. 1 (color online). (a) Schematic energy diagram of the two-electron system. Inset: false-color scanning electron micrograph image of a double dot with integrated rf QPC charge sensor similar to the one measured (scale bar is 500 nm). (b) Gate-pulse cycle that is used to prepare (P) the (2,0) singlet, separate (S) into (1,1), either to the S-T_0 degeneracy [left (green) dashed line] or the S-T_+ degeneracy [right (red) dashed line], and return to (2,0) for measurement (M). (c) rf QPC readout $V_{\rm rf}$ around the (1,1)–(2,0) transition during application of the cyclic gate-pulse sequence, showing the readout triangle indicated with white lines ($B = 0$ mT, $\tau_S = 50$ ns). A background plane has been subtracted. (d) $V_{\rm rf}$ as in (c) but for S at the S-T_+ degeneracy ($B = 10$ mT). (e) Average value of $P_S(\tau_S)$ at $B = 0$, $\tau_M = 2$ μs. Red line is a fit to the theoretical Gaussian form. (f) Average value of $P_S(\tau_M)$ showing contrast dependence, $\tau_S = 50$ ns. Red line is a fit to the exponential form (see main text).

by components of $\Delta\mathbf{B}_{\rm nuc}$ *along* the total field (applied plus Overhauser fields). In contrast, mixing of S with T_+ (the $m_s = +1$ triplet), which occurs at a less negative, field-dependent value of ϵ [right (red) dashed line in Fig. 1(b)] where Zeeman splitting matches exchange, is driven by components of $\Delta\mathbf{B}_{\rm nuc}$ *transverse* to the total field. Measuring the evolution out of the S state following separation, by measuring the return probability to (2,0) after a certain separation time, effectively measures these components of the Overhauser field difference in the two dots. Measurement (at position M) in (2,0) is made for $\tau_M = 5$ μs, during which only S return to (2,0) with appreciable probability. The spin state—triplet or singlet—is thereby converted to a charge state—(1,1) or (2,0), respectively—which is detected by the rf QPC.

Once calibrated, $V_{\rm rf}$ gives the probability $1 - P_S$ that a prepared singlet evolved into a triplet during the separation time τ_S. Inside the readout triangle [Fig. 1(c)], triplet states remain blocked in (1,1) for a time $T_1 \gg \tau_M$ [14]. Similarly, inside the rectangular region indicated in Fig. 1(d), the prepared singlet mixes with T_+ and becomes blocked in (1,1). Calibration of $V_{\rm rf}$ uses the signal in (2,0) outside the readout triangle, where fast, spin-independent relaxation occurs via (1,0) or (2,1), to define $P_S = 1$, and the region within (1,1) to define $P_S = 0$.

Fitting $P_S(\tau_S)$ averaged over tens of seconds with a Gaussian [9,13] [Fig. 1(e)] gives $T_2^* = \hbar/(g\mu_B B_{\rm nuc}) \sim 15$ ns corresponding to $B_{\rm nuc} \sim 1.6$ mT ($N \sim 6 \times 10^6$), where $g \sim -0.4$ is the electron g factor and μ_B is the Bohr magneton. The effect of finite T_1 on the calibration of P_S can be accounted by introducing a factor $C = (1 - e^{-\tau_M/T_1})T_1/\tau_M$ [14] that relates P_S to the value P_S' corresponding to infinite T_1, $1 - P_S = (1 - P_S')C$. The dependence of P_S on τ_M (for a fixed $T_1 \sim 16$ μs and $\tau_S = 50$ ns) is shown in Fig. 1(f). Applying this factor to Fig. 1(e) gives $P_S'(\tau_S \gg T_2^*) = 1/3$, the expected value [13], without normalizing the sensor output.

With less averaging, P_S shows fluctuations that reflect fluctuations of Overhauser field components. Figure 2

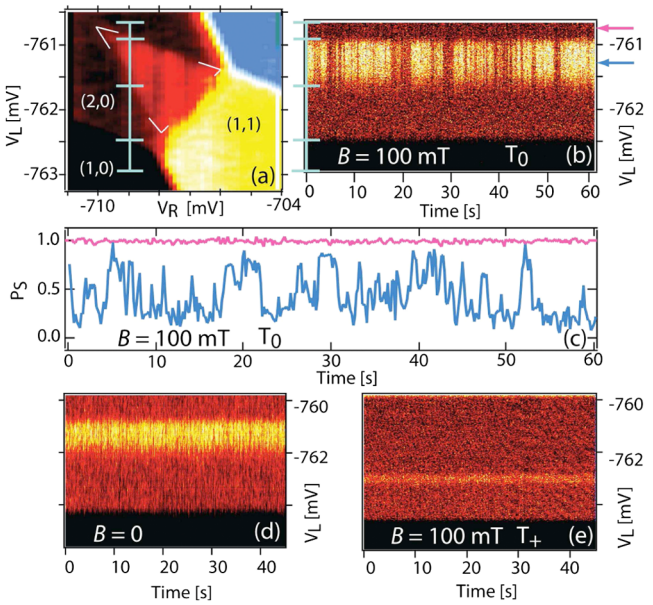

FIG. 2 (color online). (a) rf QPC sensor output $V_{\rm rf}$ as a function of V_L and V_R with gate-pulse cycle applied ($\tau_S = 25$ ns, $\tau_M = 1.6$ μs, $B = 100$ mT). Color scale as in Fig. 1. (b) Repeated slices of V_L with $V_R = -709$ mV as a function of time. Markers on left axis correspond to markers in (a). (c) Sensor output calibrated to P_S (lower, blue) along with a measurement of the background QPC noise (upper, pink) from (b) at arrow positions. Bandwidth limited to ~3 Hz. (d) Similar to (b) but for $B = 0$, color scale same as in Fig. 1. (e) Similar to (b) but with S point at S-T_+ degeneracy, $B = 100$ mT; color scale same as in Fig. 1.

shows a slice through the readout triangle, obtained by rastering V_L at fixed V_R, with $B = 100$ mT, $\tau_S = 25$ ns. At $B = 100$ mT, fluctuations in P_S have a flickering appearance with broadband time dependence extending to several seconds. Comparing the quieter (upper, pink) trace in Fig. 2(c), for point M such that (1,1) always returns to (2,0), to the fluctuating (lower, blue) trace, where return to (2,0) requires S-T_0 mixing by Overhauser fields, we see that the amplitude of the fluctuating signal (lower, blue) is ~100 times larger than the background noise of the charge sensor. At $B = 0$, slices across the readout triangle do not show a flickering (large, low-frequency) P_S signal [Fig. 2(d)]. Figure 2(e) shows slices across the S-T_+ resonance [see Fig. 1(d)]. Here also, P_S also does not have a flickering appearance, independent of B, reflecting rapid fluctuations of transverse components of $\Delta\mathbf{B}_{\mathrm{nuc}}$. We avoid rapidly cycling through the S-T_+ transition, which can produce DNP [26].

To investigate the spectral content of P_S fluctuations, fast Fourier transforms (FFTs) of V_{rf} are taken with V_L and V_R positioned to sample the center of the readout triangle. Measurement at $\tau_S = 1$ ns, where $P_S \sim 1$, has a $1/f$ form and is identical to the noise measured outside the readout triangle, and constitutes our background of instrument noise. At $B = 0$ no spectral content above the $1/f$ background noise is seen [Fig. 3(a)]. With increasing B, an increasing spectral content is observed below ~100 Hz. For $B > 20$ mT, the spectra become independent of B. The dependence of the power spectrum of P_S on separation time τ_S is shown in Fig. 4. We found that the largest fluctuations over the greatest frequency range occur for $\tau_S \sim T_2^* \sim 15$ ns, and these fluctuations show a roughly $1/f^2$ spectrum. For $\tau_S < T_2^*$, P_S remains near unity with few fluctuations; for $\tau_S > T_2^*$ low-frequency content is suppressed while components in the range 1–10 Hz are enhanced.

We model fluctuations in P_S as arising from the dynamic Overhauser magnetic field in thermal equilibrium. A classical Langevin equation is used to describe fluctuations of $\Delta\mathbf{B}_{\mathrm{nuc}}$ arising from nuclear spin diffusion on distances much larger than the lattice spacing and times much longer than the time scale set by nuclear dipole-dipole interaction. For $B \gg B_{\mathrm{nuc}}$, correlations of the Overhauser field can be evaluated analytically in terms of a dimensionless operator $\hat{A}_z^\beta$ for each nuclear spin species β, where $\sum_\beta x^\beta \hat{A}_{z,l}^\beta \equiv \mathbf{B}_{\mathrm{nuc},z}^l / B_{\mathrm{nuc}}$ and similarly for the right dot, with $x^{75\mathrm{As}} = 1$, $x^{69\mathrm{Ga}} = 0.6$, $x^{71\mathrm{As}} = 0.4$. This gives $\langle \hat{A}_z^\beta(t+\Delta t)\hat{A}_z^\beta(t)\rangle = [(1+\Delta t D_\beta/\sigma_z^2)^{1/2}(1+\Delta t D_\beta/\sigma_\perp^2)]^{-1}$, at time difference Δt, where D_β is the species-dependent spin diffusion coefficient, σ_z is the electron wave function spatial extent perpendicular to the 2DEG (and along the external field), and $\sigma_\perp$ is the wave function extent in the plane of the 2DEG, assumed symmetric in the plane. Brackets $\langle\cdots\rangle$ denote averaging over t and nuclear ensembles.

Statistics of P_S for S-T_0 mixing are found using the z component of the Overhauser operators, $\Delta\hat{A}_z = \sum_\beta x^\beta(\hat{A}_{z,l}^\beta - \hat{A}_{z,r}^\beta)$. For Gaussian fluctuations and a species-independent diffusion constant, D, this gives a mean $\langle P_S\rangle = \frac{1}{2}[1 + e^{-2G^2\langle\Delta\hat{A}_z^2\rangle}]$ and autocorrelation $\langle P_S(t+\Delta t)P_S(t)\rangle - \langle P_S\rangle^2$

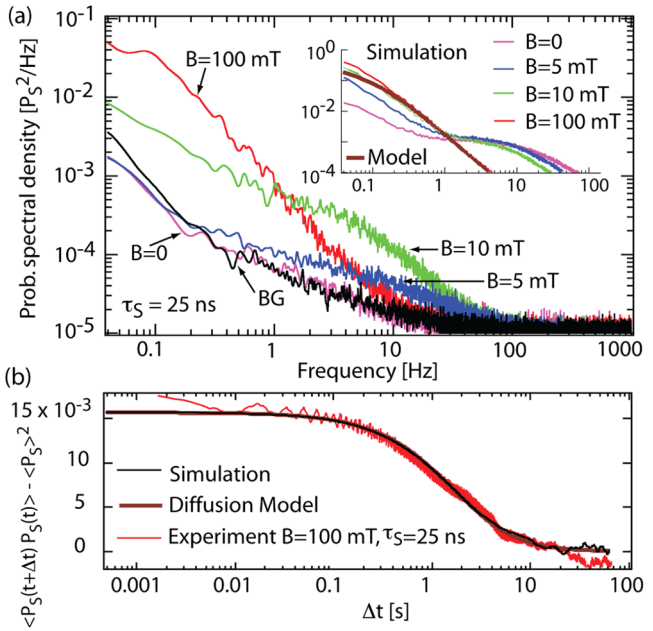

FIG. 3 (color online). (a) Power spectra of P_S at various magnetic fields, $\tau_S = 25$ ns. Spectra obtained by fast Fourier transform (with Hamming window) of average of 8 traces sampled at 10 kHz. Background measurement noise (BG) found by setting $\tau_S = 1$ ns at $B = 100$ mT. Inset: numerical simulation results for corresponding magnetic fields: $B = 0$ (pink), $B = 5$ mT (blue), $B = 10$ mT (green), $B = 100$ mT (red). (b) Autocorrelation P_S for $\tau_S = 25$ ns and $B = 100$ mT (red curve). Model function [Eq. (1)] (brown curve) and Monte Carlo result (black curve).

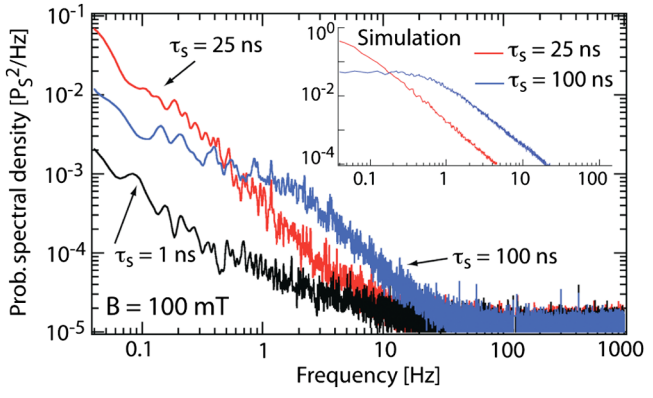

FIG. 4 (color online). Power spectra of P_S at $B = 100$ mT for separation times $\tau_S = 25$ ns (red line) and $\tau_S = 100$ ns (blue line). Setting $\tau_S = 1$ ns (black line) yields background noise. Inset shows simulation results for $B = 100$ mT, $\tau_S = 25$ ns (red) and $\tau_S = 100$ ns (blue). Note the suppression of low-frequency content and enhancement of midfrequency content for long τ_S in the experiment and simulation.

$$= \frac{e^{-4G^2\langle \Delta \hat{A}_z^2 \rangle}}{4}[\cosh(4G^2\langle \Delta \hat{A}_z(t+\Delta t)\Delta \hat{A}_z(t)\rangle) - 1], \quad (1)$$

where $G = \tau_S/T_2^*$ is a gain coefficient. Autocorrelation at $B = 100$ mT [Fig. 3(b)] is obtained by Fourier transforming the power spectrum [31], and fit to the data, with the contrast factor C [Fig. 1(f)], and the diffusion coefficient D, as fit parameters. Wave function widths are taken from numerical simulations of the device [32], $\sigma_z = 7.5$ nm, $\sigma_\perp = 40$ nm. The fit gives $D \sim 10^{-13}$ cm^2/s, consistent with previous measurements on bulk GaAs samples using optical techniques [6]. For $B > 20$ mT, the data in Fig. 3(b) indicate an autocorrelation time of $\sim$3 s for P_S corresponding to a time $\tau_d \sim 10$ s for ΔA_z to decorrelate by half of its initial value.

Near $B = 0$, transverse components of the nuclear field lead to rapid dephasing of nuclear spins. In this regime, Monte Carlo methods are used to simulate nuclear dynamics [33]. Numerical and analytical approaches agree at higher fields [Fig. 3(b)], where both methods are applicable. Numerical power spectra for $B \sim 0$ are shown in the inset of Fig. 4.

Experiment and theory show reduced low-frequency spectral content as B decreases toward zero. This can be understood as arising from the influence of the transverse nuclear fields at low B, which rapidly dephase nuclear spins and suppress long time correlations in ΔB_{nuc}. Similar behavior, though independent of B, is observed in the spectra of P_S at the S-T_+ resonance (not shown). Below $B \sim 10$ mT, an increased spectral content at frequencies between 1–10 Hz is observed in the experiment and theory. The frequency at which the spectra intersect, however, remains constant ($\sim$1 Hz) in the simulations but increases at low B in the experimental data. We are able to approximate this behavior in the simulation by increasing the diffusion coefficient ($D \sim 10^{-12}$ cm^2/s at $B = 0$), implying an enhancement of diffusion, beyond typical values [6], as B approaches zero. This may be due to the growing influence of nonsecular terms in the dipole-dipole interaction at low magnetic field [8,23]. Diffusion may be further enhanced at low B as a result of electron mediated flip-flop of nuclear spins [12,34], an effect neglected in the simulation.

Finally, we model how the separation time for the two-electron spin state affects the power spectra. Simulated spectra are shown in the inset of Fig. 4 for $\tau_S = 1$, 25, and 100 ns at $B = 100$ mT. Good agreement with experiment is achieved when again accounting for the additional $1/f$ noise and contrast reduction. We find that τ_S acts to filter fluctuations in ΔB_{nuc}, so that for $\tau_S \gg T_2^*$, low-frequency correlations in ΔB_{nuc} are suppressed in the spectra of P_S [see Eq. (1)]. This filtering effect leads to the turnover at $\sim$2 Hz evident in the spectra for $\tau_S =$ 100 ns. For $\tau_S \sim T_2^*$, little filtering occurs and the power spectra of P_S reflect the underlying intrinsic fluctuations of the Overhauser magnetic field.

We thank L. DiCarlo, A. C. Johnson, and M. Stopa for contributions. This work was supported by the Department of Defense, ARO/IARPA, NSF-NIRT (EIA-0210736), and Harvard Center for Nanoscale Systems. Research at UCSB supported in part by QuEST, a NSF Center.

*Present address: School of Physics, University of Sydney, Sydney, 2006, Australia.

[1] D. Loss and D. DiVincenzo, Phys. Rev. A **57**, 120 (1998).
[2] B. E. Kane, Nature (London) **393**, 133 (1998).
[3] S. I. Erlingsson, Y. V. Nazarov, and V. I. Fal'ko, Phys. Rev. B **64**, 195306 (2001).
[4] I. A. Merkulov, A. L. Efros, and M. Rosen, Phys. Rev. B **65**, 205309 (2002).
[5] A. V. Khaetskii, D. Loss, and L. Glazman, Phys. Rev. Lett. **88**, 186802 (2002).
[6] D. Paget, G. Lampel, and B. Sapoval, Phys. Rev. B **15**, 5780 (1977).
[7] A. S. Bracker *et al.*, Phys. Rev. Lett. **94**, 047402 (2005).
[8] R. de Sousa and S. Das Sarma, Phys. Rev. B **68**, 115322 (2003).
[9] J. R. Petta *et al.*, Science **309**, 2180 (2005).
[10] W. M. Witzel and S. Das Sarma, Phys. Rev. B **74**, 035322 (2006).
[11] F. H. L. Koppens *et al.*, Nature (London) **442**, 766 (2006).
[12] W. Yao, R.-B. Liu, and L. J. Sham, Phys. Rev. B **74**, 195301 (2006).
[13] J. M. Taylor *et al.*, Phys. Rev. B **76**, 035315 (2007).
[14] A. C. Johnson *et al.*, Nature (London) **435**, 925 (2005).
[15] F. H. L. Koppens *et al.*, Science **309**, 1346 (2005).
[16] A. K. Huttel *et al.*, Phys. Rev. B **69**, 073302 (2004).
[17] J. M. Taylor *et al.*, Nature Phys. **1**, 177 (2005).
[18] G. Giedke *et al.*, Phys. Rev. A **74**, 032316 (2006).
[19] D. Klauser, W. A. Coish, and D. Loss, Phys. Rev. B **73**, 205302 (2006).
[20] S. A. Crooker *et al.*, Nature (London) **431**, 49 (2004).
[21] T. Sleator *et al.*, Phys. Rev. Lett. **55**, 1742 (1985).
[22] C. L. Degen *et al.*, Phys. Rev. Lett. **99**, 250601 (2007).
[23] A. Abragam, *Principles of Nuclear Magnetism*, International Series of Monographs on Physics Vol. 32 (Oxford University, New York, 1983).
[24] D. Gammon *et al.*, Science **277**, 85 (1997).
[25] J. Baugh *et al.*, Phys. Rev. Lett. **99**, 096804 (2007).
[26] J. R. Petta *et al.*, Phys. Rev. Lett. **100**, 067601 (2008).
[27] K. Ono and S. Tarucha, Phys. Rev. Lett. **92**, 256803 (2004).
[28] M. S. Rudner and L. S. Levitov, Phys. Rev. Lett. **99**, 036602 (2007).
[29] O. N. Jouravlev and Y. Nazarov, Phys. Rev. Lett. **96**, 176804 (2006).
[30] D. J. Reilly *et al.*, Appl. Phys. Lett. **91**, 162101 (2007).
[31] The correlation function for the experimental data becomes slightly negative at long times, likely as the result of $1/f$ noise in the rf QPC.
[32] M. Stopa (private communication).
[33] J. M. Taylor (unpublished).
[34] C. Deng and X. Hu, Phys. Rev. B **73**, 241303(R) (2006).